Lateral Si/SiO_2 quantum well solar cells

R. Rölver,[a] B. Berghoff, D. L. Bätzner, B. Spangenberg, and H. Kurz
Institute of Semiconductor Electronics, RWTH Aachen University, Sommerfeldstraße 24, D-52074 Aachen, Germany

(Received 9 April 2008; accepted 2 May 2008; published online 28 May 2008)

The photovoltaic properties of Si/SiO_2 multiple quantum wells (QWs) embedded in lateral Schottky contacts are investigated. The QWs were fabricated by remote plasma enhanced chemical vapor deposition. By subsequent rapid thermal annealing, the two-dimensional Si layers are partially recrystallized, which gives rise to distinct quantum confinement effects. Although the current extraction along the quantum layers is hampered by the incomplete recrystallization, the data collected define the route to optimized Si based QW solar cells. © *2008 American Institute of Physics*. [DOI: 10.1063/1.2936308]

Energy conversion efficiency is the key parameter for all photovoltaic technologies since it directly impacts device and deployment costs. The efficiency of standard wafer processed solar cells is still below the theoretical limit of photovoltaic energy conversion (86%).[1]

One possibility to improve the conversion efficiency of Si based solar cells is the introduction of multiple absorbers consisting of Si/SiO_2 quantum wells (QWs).[2] In the Si/SiO_2 QW absorber material, charge carrier confinement results in effective band gap energies well above the bulk band gap of 1.1 eV, tunable by the Si QW thickness. The Si based tandem cell has a theoretical efficiency limit of 60%.[1]

Several approaches have been undertaken to fabricate high quality Si quantum structures such as Si/SiO_2 QWs (Refs. 3–5) and Si quantum dots in a SiO_2 matrix.[6–9] The band gaps in these structures are in the range of 1.1 eV (bulk Si) to 1.6 eV (Refs. 3 and 5) for QWs and 1.7 eV for crystalline quantum dots,[7] respectively. Current research also focuses on Si quantum structures embedded in alternative host matrices such as Si_3N_4 (Ref. 10) or SiC.[11]

Quantum confinement in Si nanostructures, however, rises the fundamental dilemma of sufficient charge extraction, which is necessary for efficient photovoltaic devices. Here, we try to explore the route for a possible solution by investigating one-dimensional (1D) confinement in recrystallized Si layers and the extraction of charges within the nonquantized dimensions.

This means that the carrier extraction takes place parallel to the Si/SiO_2 interfaces of two-dimensional QWs while 1D confinement is sustained in the vertical direction. It is shown, that the developed lateral contact scheme is able to provide four orders of magnitude enhanced conductivity compared to Si/SiO_2 QWs with standard vertical contacts where the charge transport is limited by insulating SiO_2 barriers.[12]

In order to analyze the optical properties, Si/SiO_2 QWs with varying layer thicknesses were deposited by remote plasma enhanced chemical vapor deposition on transparent and insulating sapphire substrates and were subsequently annealed at 1100 °C for 30 s by using rapid thermal annealing to achieve partial recrystallization. Details on the fabrication process and on the morphology of the QW material are given in Refs. 3 and 13.

Lateral contacts to the deposited Si/SiO_2 QW layers were fabricated by photolithography and subsequent reactive ion etching of 100 μm wide mesas and 80 μm square contact holes into the QW material with a pitch of 10 μm. The holes were filled with metal followed by a lift-off process, thus, defining the contact areas. For the generation of an internal electric field, adjacent contact holes were filled with Al and Pt, respectively, resulting in a Schottky barrier induced band bending. Finally, a postmetallization annealing at 400 °C for 30 min was performed, which improves the contact resistances. Dark and illuminated current voltage (*I-V*) measurements were carried out by using an HP 4156A semiconductor parameter analyzer. Photovoltaic measurements were conducted utilizing a solar simulator providing a spectrum close to the standard AM 1.5 solar irradiation (Fig. 1).

To evaluate the band gap energy of the QW material further, the optical absorption in the fabricated QWs was characterized by photothermal deflection spectroscopy (PDS).[14] Figure 2 (top) illustrates the obtained absorption spectra of Si/SiO_2 layer stacks with 1×60, 12×5, 20×3, and 30×2 nm Si wells. All of the spectra show two distinct regions of different exponential slopes separated by the band gap energy. Below the band gap, defect induced tail states within the band gap (Urbach tail) account for the absorption signal below the band gap energy.[15] For energies above the band gap, e.g., 1.14 eV for the 60 nm, 1.25 eV for the 5 nm, 1.3 eV for the 3 nm, and 1.55 eV for the 2 nm QW samples, the slope of the absorption curve increases due to the higher density of states above the energy gap. The distinct blueshift of the absorption spectra with decreasing QW thicknesses can be attributed to the quantum confinement effect.

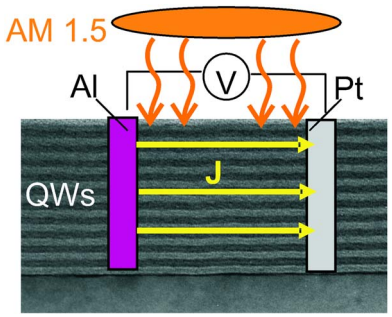

FIG. 1. (Color online) Measurement and contact scheme (cross section) of the Al/QW/Pt Schottky cell structure.

[a]Author to whom correspondence should be addressed. Electronic mail: roelver@iht.rwth-aachen.de,

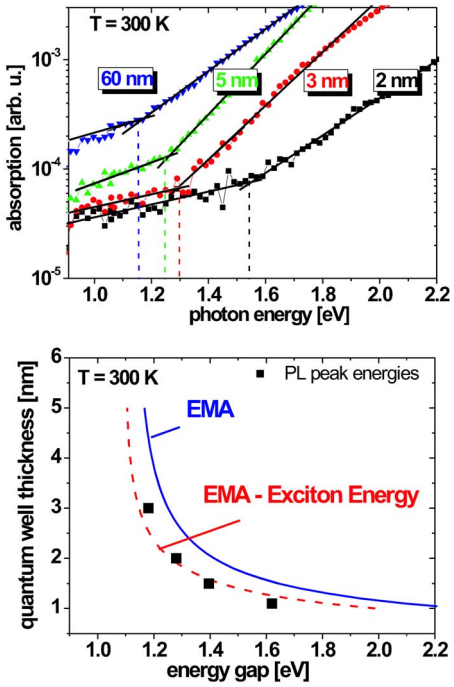

FIG. 2. (Color online) Top: PDS absorption spectra on Si/SiO_2 QWs with 3 nm SiO_2 barriers and varying Si layer thicknesses of 1×60 nm (triangles down), 12×5 nm (triangles), 20×3 nm (circles), and 30×2 nm (squares). The effective band gaps (dashed lines) are extracted from the intersection of the exponential fits of the Urbach tail below and the band to band absorption above the energy gap (solid lines). Bottom: comparison of the PL peak energies (squares) with the EMA (solid line). To regard the excitonic nature of the PL emission, the EMA model is modified by substracting the QW thickness dependent excitonic binding energy (EMA-exciton energy) (details in Ref. 3).

In addition, photoluminescence (PL) measurements have also shown the same behavior of an increase in the band gap related PL peak energy with decreasing QW thickness.[3] A comparison of the room temperature PL spectra with the well known effective mass approximation[3] (EMA) reveals a good correlation between the measured PL peak energies and the EMA model if the excitonic nature of radiative recombination is considered[3] (Fig. 2, bottom). For the calculation of the effective band gap and the excitonic binding energy the effective masses for electrons ($m_e=1.1m_0$) and holes ($m_h=0.5m_0$) known for bulk, Si were used. Both absorption and PL measurements have proven the ability to engineer the band gap in the Si/SiO_2 QW system which is needed for the implementation of an all Si tandem solar cell.

In an exploratory experiment, the QW absorber was integrated in the lateral Schottky contact based device structure. The internal electric field is generated by the work function difference $\Delta\Phi$ between the contact metals and the Si

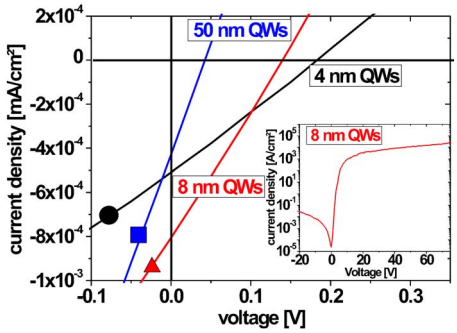

FIG. 3. (Color online) *I-V* characteristics of cell structures with varying Si QW thicknesses of 1×50 nm (square), 6×8 nm (triangle), and 12×4 nm (circle) obtained under illumination. The inset shows the diode characteristic of the 6×8 nm Pt/QW/Al structure.

QWs (theoretical values: $\Phi_{AlSi}=4.2$ eV, $\Phi_{PtSi}=5.5$ eV) resulting in the diode *I-V* characteristic shown for a Al/QW/Pt structure with 8/3 nm Si/SiO_2 QWs (Fig. 3, inset). To illustrate the performance of the fabricated solar cell devices, in Fig. 3, the *I-V* characteristics obtained under 1 sun illumination of Al/QW/Pt structures with QW thicknesses of 1×50, 6×8 nm, and 12×4 nm separated by 3 nm SiO_2 barriers is shown. To gain further insight into the differences in charge transport and energy conversion between the recrystallized QW structures and monocrystalline silicon, the photovoltaic behavior of a 30 nm monocrystalline Si layer of a silicon-on-insulator (SOI) wafer with an identical contact scheme is fabricated and characterized in the same way as the QW devices (see Table I).

As demonstrated in Fig. 3, the embedded QW samples exhibit photovoltaic behavior. The obtained *I-V* curves are linear, i.e., the current voltage characteristics are dominated by the series resistances R_S (R_S values determined from the slope of the *I-V* characteristic are shown in Table I). The increase in R_S in the QW samples compared to the single crystalline SOI layer is attributed to amorphous grain boundaries limiting the current transport in the recrystallized QW material. The further increase in R_S with reduced QW thickness between 50 nm QW and 4 nm QW is related to the decrease in crystallinity of the Si layers, i.e., 90% in the 50 nm Si layers and only 10% in the 4 nm QWs, as determined by Raman measurements.[16] Due to the high series resistances, the short circuit currents are limited to 2×10^{-2} mA/cm^2 for the SOI reference and to the 10^{-4} mA/cm^2 range for the QW samples.

Furthermore, the open circuit voltages V_{oc} raise if the Si QW thickness is reduced. As shown in Table I, V_{oc} increases from 20 mV in the SOI sample and 40 mV in the 50 nm QW to 191 mV in the 4 nm QW sample. This enhancement can

TABLE I. Comparison of the measured (M) and calculated (C) V_{oc} and J_{sc} values in the Al/QW/Pt-Schottky cell structures with varying QW thicknesses d_{Si}. The parameters needed for the calculation of J_{sc}^C and V_{oc}^C, the barrier height $q\Phi_B$, the photocurrent J_{ph}, and the series resistance R_s are also shown.

d_{Si} (nm)	$q\Phi_B$ (eV)	J_{ph} (mA/cm^2)	R_s (kΩ)	V_{oc}^M/V_{oc}^C (mV)	J_{sc}^M/J_{sc}^C (10^{-4} mA/cm^2)
30 SOI	0.56	5	1	20/14	200/220
50	0.56	14	93	40/40	4.3/4.8
8	0.63	12	141	114/110	8.1/8
4	0.71	10	374	191/185	5.1/3.6

be directly attributed to the increase in the band gap energy in ultrathin QWs. With increasing band gap, the difference between the Fermi level and conduction band E_C-E_F as well as between the Fermi level and valence band E_V-E_F grows. As a consequence, the Schottky barrier height $q\Phi_B$ at both contacts increases, which reduces the reverse currents J_R in the Schottky contact QW cells according to the thermionic emission formula[17]

$$J_R = A^* T^2 \exp\left(-\frac{q\Phi_B}{kT}\right), \tag{1}$$

with the effective Richardson constant A^*, the temperature T, and the Boltzmann constant k. The relation between reverse current J_R and open circuit voltage V_{oc} is then

$$V_{oc} \cong \frac{kT}{q} \ln\left(\frac{J_{ph}}{J_R}\right) = \Phi_B - \ln\left(\frac{A^* T^2}{J_{ph}}\right), \tag{2}$$

with the photocurrent density J_{ph}. Assuming every photon generates an electron hole pair contributing to the photocurrent, the theoretical dependence of V_{oc} from the band gap using Eqs. (1) and (2) have been calculated by using literature values for the Richardson constant for electrons (A^* $=120$ A cm^{-2} K^{-2}) and holes ($A^*=40$ A cm^{-2} K^{-2}).[17] For the SOI and the 50 nm Schottky cell structure, a barrier height $q\Phi_B$ of 0.56 eV for the band offsets at the Al/Si and the Pt/Si interface has been found in accordance with literature values summarized in Ref. 17. For the samples with QW thicknesses below 50 nm, the band gap shift ΔE_G extracted from the PDS measurements was added to the barrier height values $q\Phi_B$ found for the metal/bulk-Si interface. For a first estimate, we considered the Schottky barriers to increase equally for the valence and conduction bands leading to an overall growth of the barrier height at both contacts by 0.5 $\times \Delta E_G$. In addition, the ideal photocurrent density J_{ph} for all samples is calculated by convoluting the measured (QW samples) or known bulk Si (Ref. 17) (SOI sample) absorption spectra and the AM 1.5 solar spectrum. In Table I, the measured and calculated photovoltaic parameters are compared and summarized. The excellent agreement between measured and calculated V_{oc} values shown in Table I supports the conclusion that V_{oc} rises due to a quantum confinement induced shift of the band gap. Furthermore, the apparently low V_{oc} values in the samples investigated are a direct consequence of high reverse currents in the Schottky contact solar cells as well as the low absorption limiting the theoretically obtainable photocurrent density J_{ph}.

As mentioned above, J_{sc} is mainly determined by the high series resistances. According to the one diode model,[18] the short circuit current ($V=0$) is given by

$$J_{sc} = J_R\left[\exp\left(-\frac{J_{sc}R_S}{kT}\right) - 1\right] - J_{ph}, \tag{3}$$

applying the same parameters J_R, R_S, and J_{ph} already used for the calculation of V_{oc}. There is a convincing agreement between the measured and calculated J_{sc} values supporting the validity of a Schottky barrier induced electric field as a driving force in this solar cell structure.

The data collected in Table I demonstrates that the high series resistances along with the insufficient absorption limiting J_{ph} are the main obstacles for a more pronounced benefit of quantum size effects in the fabricated QW based solar cells so far. The principle idea to separate the directions of confinement and extraction seems to be confirmed.

In conclusion, Si QW solar cells were developed by using a lateral transport concept along with an internal field provided by Schottky contacts. It is shown, that the open circuit voltage, and thus, conversion efficiency can be enhanced due to confinement effects in a Si based QW absorber. Although in this preliminary work the lateral conductivity is still too low for efficient photovoltaic energy conversion, the path to an improved QW solar cell is quite clear. An optimized lateral device should comprise of fully recrystallized and weakly doped QWs to minimize series resistance and highly doped polycrystalline silicon instead of Schottky contacts resulting in a *p-i-n* structure to minimize reverse currents which should yield V_{oc} values potentially above those of standard Si solar cells. For optimum efficiency of the desired QW/bulk Si tandem cell, the number of Si layers needs to be adjusted in such a way, that identical photocurrents J_{ph} are obtained for the QW absorber and the underlying bulk Si. With these optimizations, it should be possible to benefit from the quantum confinement in fully recrystallized Si layers, which represents a major development toward highly efficient all silicon tandem solar cells.

We thank J. Klomfass, T. Kirchartz, and U. Rau (FZ Jülich) for valuable discussions and PDS measurements and T. Arguirov and T. Mchedlidze (BTU Cottbus) for the Raman analysis. Financial support was provided by the BMBF, Germany (Contract No. 03SF0308A) and by the MIWFT NRW.

[1] M. A. Green, *Third Generation Photovoltaics* (Springer, Berlin, 2003).
[2] M. A. Green, Mater. Sci. Eng., B **74**, 118 (2000).
[3] R. Rölver, M. Först, O. Winkler, B. Spangenberg, and H. Kurz, J. Vac. Sci. Technol. A **24**, 141 (2006).
[4] D. J. Lockwood, Z. H. Lu, and J. M. Barribeau, Phys. Rev. Lett. **76**, 539 (1996).
[5] V. Vinciguerra, G. Franzo, F. Priolo, F. Iacona, and C. Spinella, J. Appl. Phys. **87**, 8165 (2000).
[6] J. Ruan, P. M. Fauchet, L. Dal Negro, M. Cazzanelli, and L. Pavesi, Appl. Phys. Lett. **83**, 5479 (2003).
[7] M. Zacharias, J. Heitmann, R. Scholz, U. Kahler, M. Schmidt, and J. Bläsing, Appl. Phys. Lett. **80**, 661 (2002).
[8] M. L. Brongersma, P. G. Kik, A. Polman, K. S. Min, and H. A. Atwater, Appl. Phys. Lett. **76**, 351 (2000).
[9] J. Heitmann, F. Müller, L. Yi, M. Zacharias, and F. Eichhorn, Phys. Rev. B **69**, 195309 (2004).
[10] L. Van Dao, J. Davis, P. Hannaford, Y. H. Cho, M. A. Green, and E. C. Cho, Appl. Phys. Lett. **90**, 081105 (2007).
[11] D. Song, E. C. Cho, G. Conibeer, Y. Huang, S. Huang, C. Flynn, and M. A. Green, J. Vac. Sci. Technol. B **25**, 1327 (2007).
[12] R. Rölver, B. Berghoff, D. Bätzner, B. Spangenberg, H. Kurz, B. Stegemann, and M. Schmidt, "*Si/SiO$_2$ multiple quantum wells for silicon tandem cells: Conductivity and photocurrent measurements*," Thin Solid Films (in press).
[13] R. Rölver, O. Winkler, M. Först, B. Spangenberg, and H. Kurz, Microelectron. Reliab. **45**, 915 (2005).
[14] J. Sancho-Porramon, J. Ferre-Borull, S. Bosch, A. Krasilnikova, and J. Bulir, Appl. Surf. Sci. **253**, 158 (2006).
[15] F. Urbach, Phys. Rev. **92**, 1324 (1953).
[16] T. Arguirov, T. Mchedlidze, M. Kittler, R. Rölver, B. Berghoff, M. Först, and B. Spangenberg, Appl. Phys. Lett. **89**, 05311 (2006).
[17] S. M. Sze, *Physics of Semiconductor Devices* (Wiley, New York, 1981).
[18] P. Würfel, *Physik der Solarzellen* (Spektrum, Heidelberg, 2000).